In-situ geotechnical investigations for evaluating static liquefaction potential of mine tailings

Ali Reza Zafarani, Mireille Sandrine Ewane, Amir Hossein Zamani & Philip Gomes
Sustainable Mining Development Department, SNC-Lavalin, Montréal, Québec, Canada
Jean-François Painchaud
Newmont Corporation, Éléonore Mine, James Bay, Québec, Canada

ABSTRACT
The geotechnical stability of tailings storage facilities (TSFs) has obtained considerable attention in recent years, as these facilities have been documented to fail due to flow liquefaction. Stacking of filtered tailings is currently being proposed as an alternate solution for tailings storage facilities; nevertheless, there are several challenges in identifying and analyzing these structures, especially in sites with high disposal rates. Piezocone (CPTu) testing is generally recognized as an effective tool for determining the in-situ engineering properties of tailings for use in stability and liquefaction assessments. To correlate the results of piezocone testing to liquefaction potential, several empirical approaches have been proposed. In this paper, a detailed geotechnical characterization of the tailings at the Éléonore Mine filtered tailings storage facility, located in northwest Quebec, is presented to evaluate the tailings liquefaction susceptibility under static loading condition. The analysis includes soil behaviour classification using CPTu test results, as well as static liquefaction and post-liquefaction stability analysis. The liquefaction susceptibility analysis is based on characteristics such as the Soil Behaviour Type (SBT), the State Parameter (ψ) and normalized corrected tip resistance (q_{c1}), which were calculated using a set of published empirical calibrations. According to the soil behaviour classification, the majority of tailings at various depths of the TSF exhibit dilative behaviour. The stability analyses were carried out by assigning the peak and residual undrained shear strength to the contractive layers defined by the three different classification methods. The results confirm the global safety of the TSF against static liquefaction, although for some configurations, there is a superficial critical slip surface near the toe of the TSF.

RÉSUMÉ
La stabilité géotechnique des installations de stockage des résidus (ISR) a fait l'objet d'une attention considérable ces dernières années, car il a été démontré que ces installations se rompent en raison de la liquéfaction par écoulement. L'empilement des résidus filtrés est actuellement proposé comme une solution alternative aux installations de stockage des résidus; cependant, l'identification et l'analyse de ces structures à empilement de résidus filtrés présentent plusieurs défis, particulièrement dans les sites à fort taux de stockage. L'essai au piézocône (CPTu) est généralement reconnu comme étant un outil efficace pour déterminer les propriétés techniques in situ des résidus à utiliser dans les évaluations de stabilité et de liquéfaction. Pour corréler les résultats des essais au piézocône au potentiel de liquéfaction, plusieurs approches empiriques ont été proposées. Dans cet article, une caractérisation géotechnique détaillée des résidus du bassin à résidus filtrés de la mine Éléonore, situé dans le nord-ouest du Québec, est présentée afin d'évaluer la susceptibilité à la liquéfaction des résidus sous des conditions de chargement statique. L'analyse comprend la classification du comportement du sol à l'aide des résultats des tests CPTu, ainsi que l'analyse de la stabilité du déclenchement et du post-déclenchement. L'analyse de la susceptibilité à la liquéfaction se concentre sur les caractéristiques telles que le type de comportement du sol (SBT), le paramètre d'état (ψ) et la résistance de pointe corrigée normalisée (q_{c1}), qui ont été calculées à l'aide d'un ensemble d'étalonnages empiriques publiés. Selon la classification du comportement du sol, la majorité des résidus à différentes profondeurs du ISR présentent un comportement dilatant. Les analyses de stabilité sont réalisées en attribuant la résistance au cisaillement non drainé pic et résiduelle aux couches contractives définies par trois méthodes de classification différentes. Les résultats confirment la sécurité globale du ISR contre la liquéfaction statique, bien que pour certaines configurations particulières, il existe une surface de glissement critique superficielle près du pied du ISR.

1 INTRODUCTION

Soil liquefaction occurs when the pore water pressure equals or exceeds the effective confining stress in the contractive soils, resulting in a sudden loss of shear strength. When soil particles are in a loose condition and are subjected to shearing stresses, if the pore water is not allowed to drain, it will tend to increase in response to the shearing stress, causing stresses to be transferred from the soil skeleton to the pore water, resulting in a reduction in effective stress and the shear strength of the soil. If the resistance of the soil falls below the driving shear stress, significant deformation and liquefaction can occur suddenly (Robertson and Wride, 1998; Rauch, 1997).

The identification of the soil conditions prone to flow liquefaction can be accomplished using a combination of high-quality sampling and comprehensive laboratory testing, as well as in-situ testing and geophysical

measurements (Poulos et al., 1985; Ishihara, 1993; Olson & Stark, 2003). The soil liquefaction assessment using the in-situ test data is based on empirical approaches that correlate corrected resistance measurements from SPT and CPT tests with liquefaction failure observations from case histories (Seed et al., 1985; Ishihara, 1993; Olson 2001, Olson and Stark, 2003; Idriss and Boulanger, 2008, 2014).

This paper details a method for determining the static liquefaction susceptibility of mine tailings based on in-situ test results. The methodology consists of the following steps: (1) identify contractive soil layers susceptible to liquefaction using different known criteria: (a) Plewes et al. (1992), (b) Robertson (2010, 2016 and 2022), and (c) Fear and Robertson (1995); (2) performing stability analysis using the peak undrained shear strength for the contractive layer; and (3) conducting post-liquefaction stability analysis by assigning the residual undrained shear strength to the layers more susceptible to liquefaction.

2 STUDY SITE INFORMATION

The Éléonore Mine, which is owned by Newmont Corporation since 2019, is in the James Bay region, approximately 190 kilometers east of the Cree community of Wemindji and 350 kilometers north of the town of Matagami. This gold mine has been in operation since October 2014 and is scheduled to close in 2026. The site consists of a tailings storage facility that, in its final layout, will have a footprint of about 80 hectares. As indicated in Figure 1, three (3) deposition phases are currently planned. Phase 1 has been completed and Phase 2, and 3A are in operation. A collection pond and a waste rock pile are also part of the TSF.

The processing plant includes a sulfide flotation stage, producing a sulfide concentrate representing 8% of the tailings. The sulfide tailings (8%) and 30% of the desulphurized tailings are returned underground as paste backfill.

Figure 1. The Éléonore TSF layout, 2021

The remaining 70% of the desulphurized tailings is filtered to 84% solids content and trucked to the TSF for storage. The TSF pad is lined with a high-density polyethylene (HDPE) geomembrane with Level A waterproofing measures in accordance with Québec Directive 019 (D019, 2012).

Two critical and representative sections of the Phase 1 of the TSF were selected for the stability analyses. Figure 2 illustrates the plan view of the Phase 1 of the TSF and the location of the selected sections (A-A and B-B). These sections have the greatest heights defined as the difference in elevation between the crest of the tailings pile and the downstream toe of the starter dam.

In recent years, the TSF has been the focus of various geotechnical investigations (Golder, 2009, 2010; SNC-Lavalin, 2011, 2019, 2021). The findings of these investigations and the most recent geotechnical study, completed in November 2021 (SNC-Lavalin, 2021), were employed for this analysis. This program involved seven (7) piezocone (CPT and SCPTu) penetration tests in Phase 1 of the TSF. CPT-04A-21, SCPTu-04-21, SCPTu-03-21, SCPTu-02-21, and CPT-02A-21 are near Section B-B, whereas CPT-01A-21 and CPT-01-21 are on the east side of section A-A, as shown on Figure 2. The data from these piezocones are used in this study to assess the stability of the TSF against static liquefaction.

3 METHODOLOGY AND STABILITY CRITERIA

The data collected from the CPT and SCPTu tests were used to conduct the study of the liquefaction potential of Phase 1. Figure 3 shows the flow chart of the methodology followed in this study. This study was organized into three steps: (1) soil characterization to determine the contractive and dilative zones; (2) stability analysis using the peak undrained shear strength for contractive layer; and (3) post-liquefaction stability analysis using residual undrained shear strength for layers more susceptible to liquefaction. These steps are outlined in further detail below.

3.1 Classification of the Tailings

When soil particles are in a loose (contractive) state, there is a greater chance of excess pore water pressure building up and a reduction in effective stress under shear loading. As a result, the contractive tailings layers must be defined in the initial step of the liquefaction susceptibility study. Different criteria, proposed by Plewes et al. (1992), Robertson (2010, 2016 and 2022), and Fear and Robertson (1995), are employed to characterize the state of the tailings in this study. These methods are briefly described below.

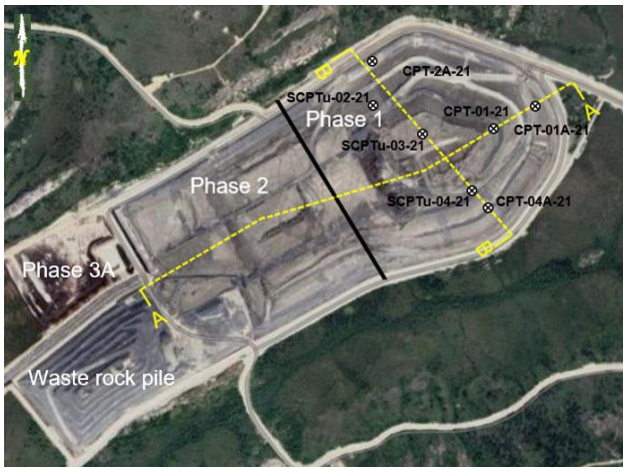

Figure 2. Plan view of the Phase 1 of the Éléonore Mine TSF with selected sections

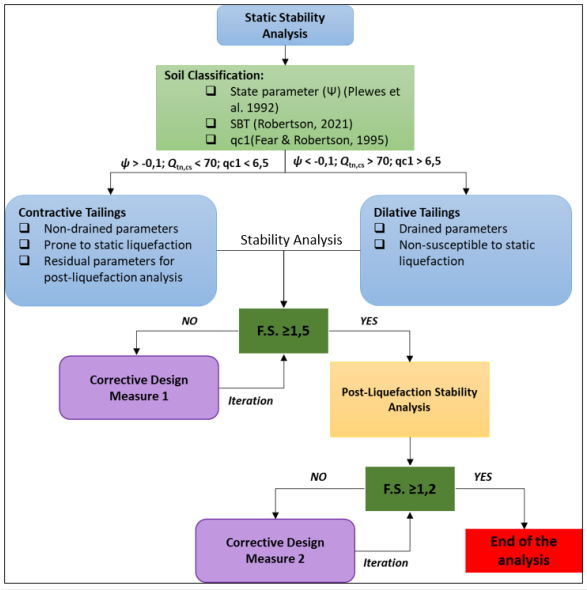

Figure 3. Flow chart of methodology used for the static liquefaction analysis

3.1.1 State Parameter (ψ) and Soil Behaviour Type (*SBT*) Charts

The state parameter (ψ) is defined as the difference between the initial void ratio (e_0) and the void ratio at critical state (e_{cs}) at shearing under constant confining stress (Plewes et al., 1992).

The use of a state parameter is essential since it helps to explain concepts such as drained and undrained soil properties, contractive or dilative behaviour, and positive versus negative porewater pressures, as well as establishing the initial state, which is frequently described in terms of relative density of the soil. Plewes et al. (1992) proposed a method based on the state parameter (ψ) to classify the soils into contractive or dilative zones. According to this method, if the state parameter is more than -0.1 ($-0.1 < \psi$), the soil is in a contractive state and there is a risk of subsequent liquefaction.

Robertson (2010) further developed a method for material behaviour classification that uses soil behaviour type (SBT) charts, which is one of the most widely used approaches. Robertson (2010) established an equation for defining the state parameter based on normalized cone tip resistance parameter, $Q_{tn,cs}$:

$$\psi = 0.56 - 0.33\, log(Q_{tn,cs}) \quad [1]$$

Where $Q_{tn,cs}$ is defined by the following equation:

$$Q_{tn,cs} = K_c \times \left(\frac{q_t - \sigma_{v0}}{P_a}\right) \times \left(\frac{P_a}{\sigma'_{v0}}\right)^n \quad [2]$$

Where q_t is the cone tip resistance, σ_{v0} is total vertical stress, σ'_{v0} is the effective vertical stress, P_a is the atmospheric pressure, n is the stress exponent which varies from 1 in intact clays to around 0.5 in sands (Robertson, 2010), and K_c is the correction factor to convert the normalized cone tip resistance of silty sands to an equivalent parameter for clean sands depending on the fines content, minerology, and plasticity of the soil (Robertson and Wride, 1998). According to Robertson (2010), the value of $Q_{tn,cs}$ equal to 70 (i.e., ψ=-0.05) can be considered as the boundary value delimiting contractive from dilative zones. When $Q_{tn,cs}$falls below 70 ($-0.05 < \psi$), the soil is said to be in loose state and prone to static liquefaction. Otherwise, it shows dilative behaviour and there is no risk of flow liquefaction.

In the present study, the two proposed criteria of Plewes et al. (1992) and Robertson (2010) are used to compare the stability analysis results in terms of the factor of safety. The zones with $-0.1 < \psi$ and $Q_{tn,cs} < 70$ will be characterized as contractive material, as shown in Figure 3.

3.1.2 Corrected Cone Tip Resistance (q_{c1})

In addition to the state parameter and $Q_{tn,cs}$, Fear and Robertson (1995), and Olson and Stark (2003) proposed a method to determine contractive and dilative zones by correlations between overburden-stress normalized penetration resistance and vertical effective stress. According to this approach, the corrected cone tip resistance, q_{c1}, is defined as $q_{c1} = q_c . C_q$, where q_c is the cone resistance and C_q is the CPT-based overburden correction factor.

Pirete and Gomes (2013) developed the following classification framework for q_{c1} using the results provided by Olson and Stark (2003):

- q_{c1} > 6.5 MPa: Zones without liquefaction potential.
- 3.25 ≤ q_{c1} ≤ 6.5 MPa: Zones with medium strength against liquefaction.
- q_{c1} < 3.25 MPa: Zones with low strength against liquefaction.

The value of q_{c1}=6.5 is used as the third criterion in this study to define the boundary between contractive and dilative behaviour.

3.2 Performing Stability Analysis

Following the determination of contractive zones, the geotechnical stability of the TSF is evaluated by assigning the peak undrained shear strength to the contractive layers susceptible to liquefaction. The Slope/W software, version 2021 of the GEOSLOPE International Ltd is used to perform the stability analysis. The methods used for this purpose are the limit equilibrium and slice methods (Morgenstern-Price, 1965), where the safety factors are obtained by relating the resisting forces to the driving forces.

To satisfy the Canadian Dam Association's guidelines for mining dams (CDA, 2019), the safety factor of FS=1.5 is targeted in this step. Corrective design measures such as stabilization berms may be considered if the safety factor is less than or equal to 1.5 (FS≤1.5).

3.3 Post-Liquefaction Stability Analysis

The final step in the liquefaction stability analysis includes assigning the residual undrained shear strength parameters to the layers most susceptible to liquefaction, i.e., all contractive layers beneath the water table and the first contractive layer above the water table. Post-liquefaction stability analyses are also performed using the Slope/W software. The analysis methods and slip surface options used are the same as described in the previous section.

Based on the safety factor, the post-liquefaction stability is determined. Thus, if the factor of safety defined by the static post-liquefaction stability analysis is less than or equal to 1.2 (FS ≤ 1.2), failure is likely. To increase the safety of the TSF, stability control elements such as stabilization berms may be constructed. However, if the factor of safety exceeds 1.2 (FS > 1.2), failure is unlikely.

4 STABILITY ANALYSES

4.1 Determination of Contractive and Dilative Behaviour

As outlined, the first step in evaluating the liquefaction potential is to perform a susceptibility analysis using ψ, $Q_{tn,cs}$ and q_{c1} parameters to determine whether the tailings are susceptible to undrained strain-softening behaviour and flow failure (contractive or dilative behaviour). These parameters are obtained from the CPT and SCPTu data. In the Phase 1 of the TSF, seven (7) piezocone tests (CPT and SCPTu) were performed. Table 1 presents the summary of these piezocone tests. Sounding depths ranged from 10 to 37.5 m. The groundwater level was measured at each in-situ test location and was found to be at an average elevation of 228 m.

Figure 4 illustrates the results of the soil classification in three plots: (a) the state parameter (ψ), (b) the corrected normalized cone tip resistance parameter ($Q_{tn,cs}$), and (c) the corrected cone tip resistance (q_{c1}). To clearly delineate field conditions that are vulnerable to flow liquefaction, the contractive zone is illustrated in red, while the dilative zone is displayed in green. The boundary between these two zones is identified using the criteria discussed in Section 3-1.

Table 1. Characteristics of piezocone tests

Piezocone Tests	Surface Elevation (m)	Water Table Elevation (m)	Borehole Depth (m)
CPT-01-21	247.5	227.6	25.4
CPT-01A-21	232.1	227.6	9.8
SCPTu-02-21	246.5	225.5	20.6
CPT-02A-21	236.5	225,5	9.7
SCPTu-03-21	260.0	229.4	37.5
SCPTu-04-21	245,5	230.2	20.5
CPT-04A-21	235.5	230.2	10.0

There are contractive zones prone to liquefaction according to the three classification methods, as shown in Figure 4. However, the variation of the ψ and $Q_{tn,cs}$ parameters versus depth (Figure 4a and Figure 4b) shows significantly more limited layers in the contractive zone compared to q_{c1} (Figure 4c). For example, the ψ and $Q_{tn,cs}$ plots reveal that for elevations ranging from 222 to 225 m, only the soil layers at 223 m are prone to flow liquefaction. However, majority of the layers in this elevation range demonstrate contractive behaviour based on the q_{c1} values. For some depth ranges, such as layers between elevations of 240 and 245 m, the three parameters give identical results. This analysis will be further discussed by comparing the results of the stability analysis using each of these classification parameters (i.e., ψ, $Q_{tn,cs}$, and q_{c1}).

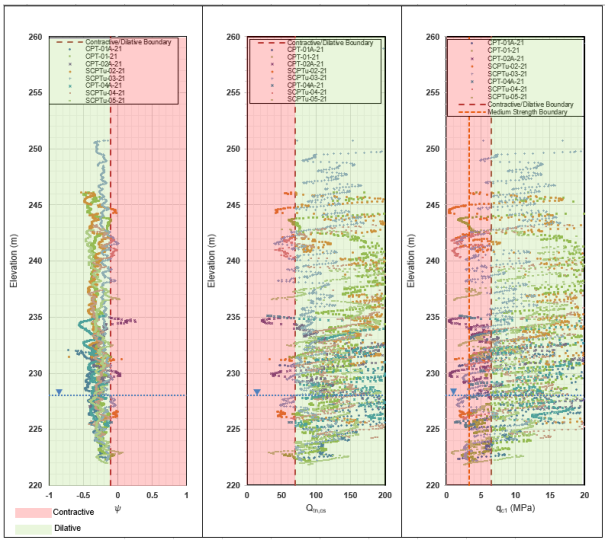

Figure 4. Variation of (a) ψ, (b) $Q_{tn,cs}$, and (c) q_{c1} versus depth for the piezocone tests presented in Table 1

4.2 Model Geometry

Following the determination of the contractive zones, the geotechnical stability of the TSF was evaluated using the limit equilibrium method in the Slope/W software. Figure 5 shows the model geometry along the cross-section B-B with the location of the piezocone tests, and the distribution of material zones determined by the ψ (Figure 5a), $Q_{tn,cs}$ (Figure 5b), and q_{c1} (Figure 5c) parameters.

The starter dike at the TSF perimeter is constructed using mine waste rock. The crest width of the starter dike is 10 m on the south side and 16 m on the north side with an average height of 4 m. The TSF pad has a 1.5 mm thick geomembrane lining. A 10-m-thick layer of impervious bedrock is added beneath the TSF. The height of the model at the crest is around 41 m. The global slope of the TSF is 5H:1V, which includes benches with a height of 10 m and a width of 10 m.

The contractive layers (shown in brown color in Figure 5) are defined using the data presented in Figure 4. It should be noted that the contractive layers are commonly considered to be continuous across the section. This assumption may be conservative for zones where CPT tests were not performed. As discussed in the previous section, classification using the ψ (Figure 5a) and $Q_{tn,cs}$ (Figure 5b) parameters results in similar contractive zones, which are limited compared to contractive zones obtained using the q_{c1} parameter (Figure 5c). The results of the static stability analysis will be discussed in the following paragraphs to investigate how the different classification criteria affect the overall stability of the tailings stack.

4.3 Material Properties

The mechanical properties used in the stability analyses are listed in Table 2. These parameters were chosen based on the results of the previous site geotechnical investigations (Golder, 2010; SNC-Lavalin, 2011, 2020b, and 2021).

The peak undrained shear strength ratio ($\frac{Su_{(peak)}}{\sigma'_{v0}}$) of the layers susceptible to static liquefaction (i.e., contractive layers) are defined using Olson's (2001) relationship:

$$\frac{Su_{(peak)}}{\sigma'_{v0}} = 0.205 + 0.0143.q_{c1}; q_{c1} \leq 6.5\ MPa \quad [3]$$

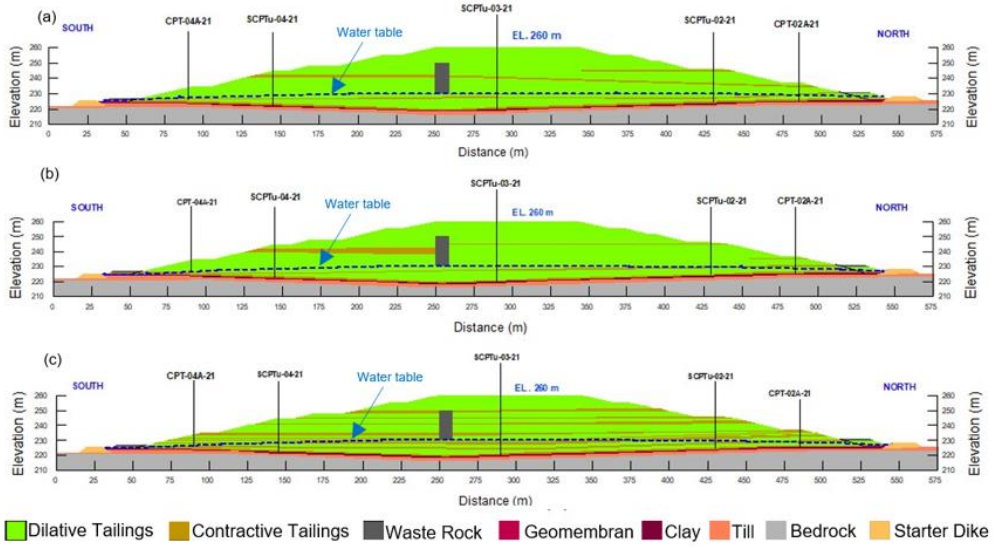

Figure 5. Model geometry along the cross-section B-B with material zoning defined by (a) ψ, (b) $Q_{tn,cs}$, and (c) q_{c1} parameters

Where $Su_{(peak)}$ is the peak undrained shear strength, σ'_{v0} is the initial effective vertical stress, and q_{c1} is the correct cone tip resistance. According to the results of the CPT and SCPTu tests, the peak undrained shear strength ratio ranges from 0.2 to 0.28. For the stability analyses, the $\frac{Su_{(peak)}}{\sigma'_{v0}}$ value of 0.22 was chosen, with a minimum Su value of 10 kPa.

The residual undrained shear strength ratio ($\frac{Su_{(Liquified)}}{\sigma'_{v0}}$) is defined using the equation proposed by Idriss et Boulanger (2008):

$$\frac{Su_{(Liquified)}}{\sigma'_{v0}} = exp\left(\frac{q_{c1}N_{cs}}{24,5} - \left(\frac{q_{c1}N_{cs}}{61,7}\right)^2 + \left(\frac{q_{c1}N_{cs}}{106}\right)^3 - 4,42\right) \leq tan\phi' \quad [4]$$

Where $Su_{(Liquified)}$ is the residual undrained shear strength, $q_{c1}N_{cs}$ is the normalized, clean sand-corrected cone tip resistance, and ϕ' is the drained internal friction angle. Based on the CPT and SCPTu measurements, an average value of 0.09 with a minimum Su value of 5 kPa is selected for the residual undrained shear strength ratio.

Table 2. Material properties

Material	Dry unit weight (kN/m³)	Internal friction angle, φ' (°)	Effective cohesion, c' (kPa)	$\frac{Su_{(peak)}}{\sigma'_{v0}}$	$\frac{Su_{(Liquified)}}{\sigma'_{v0}}$
Dilative Tailings	18	30	0	--	
Contractive Tailings	18	--	--	0.22*	--
Liquified Tailings	18	--	--	--	0.09**
Starter Dike (mine rock)	21	38	0	--	
Geomembrane	0.1	15	0	--	
Clay	16.5	23	16	--	
Till	22	33	0	--	
Bedrock	--		Impenetrable		

Note: * The minimum S_u value = 10 kPa
** The minimum S_u value = 5 kPa

5 RESULTS

5.1 Liquefaction Stability Results

Limit equilibrium stability assessments were carried out using the Morgenstern-Price method (1965) based on the model geometry of the reference section of B-B of the TSF obtained from CPT and SCPTu test results. The contractive layers in the stability analysis are defined based on the three ψ, $Q_{tn,cs}$, and q_{c1} parameters. The peak undrained shear strength ratio ($\frac{Su_{(peak)}}{\sigma'_{v0}}$) of 0.22 is assigned to the contractive zones.

Figure 6 illustrates the stability analysis results, with the contractive layers defined by (a) ψ, (b), $Q_{tn,cs}$, and (c) q_{c1} parameters. The safety factor of critical failure surface is greater than 1.5 for all classification methods on both sides of the model (i.e., south and north). Figure 6a shows that for the section classified by ψ parameter, the factor of safety of the critical failure surface on the south side is equal to 1.60, which is close to the computed values of the critical factor of safety for the models classified by $Q_{tn,cs}$, and q_{c1} parameters. The critical slip surface is generally limited to the toe area, except for the north side of the model classified using the ψ parameter, where the slip surface lies at an elevation of 235 to 245 m.

The global factor of safety computed for the model classified by ψ (Figure 6a) is close to 2.90 for both sides of the model. This is higher than the computed values for the models classified by $Q_{tn,cs}$, (Figure 6b) and q_{c1} (Figure 6c). This was expected given the low volume of contractive layers compared to the other two methods. However, the effect is less pronounced on the critical sliding surface.

5.2 Post-Liquefaction Stability Results

The post-liquefaction stability of the model is investigated in the final step of this study by assigning the residual undrained shear strength ratio ($\frac{Su_{(Liquified)}}{\sigma'_{v0}}$) to the layers most susceptible to liquefaction, which include all contractive layers beneath the water table and the first contracting layer above the water table.

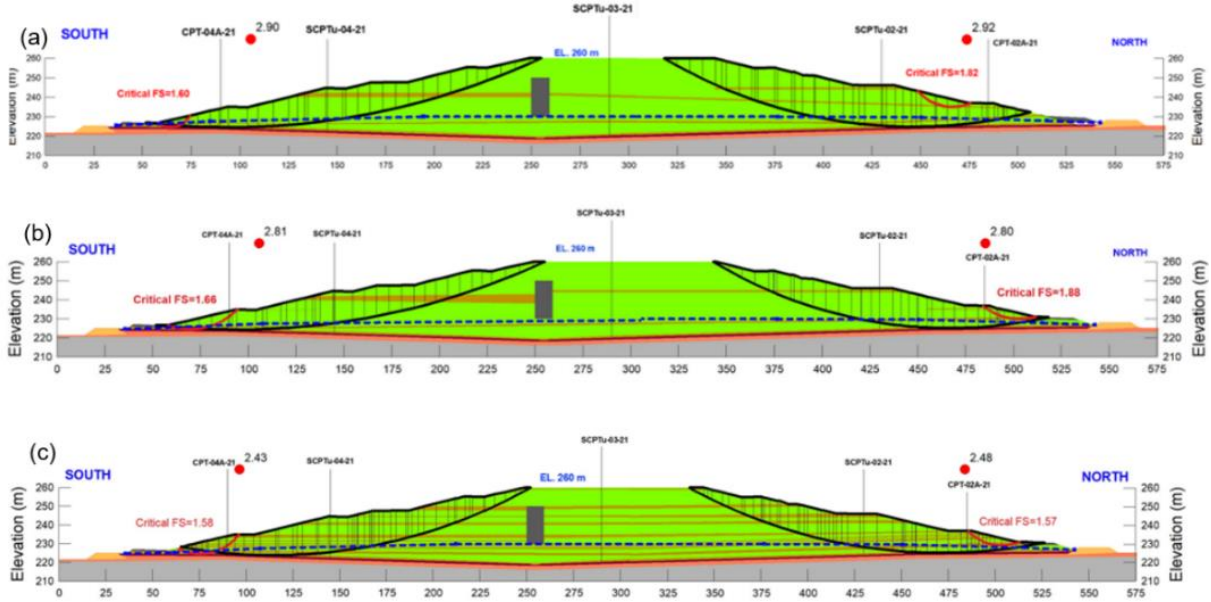

Figure 6. Liquefaction stability results along the cross-section B-B with material zoning defined by (a) ψ, (b) $Q_{tn,cs}$, and (c) q_{c1} parameters

Figure 7 shows the results of the post-liquefaction analysis for the cross-section B-B with material zoning determined by three classification criteria: (a) ψ, (b) $Q_{tn,cs}$, and (c) q_{c1}. In comparison to the liquefaction analysis, the factor of safety of the critical and global sliding surfaces decreased. For an example, the critical factor of safety at the south side of the model characterized by state parameter decreased from 1.60 (Figure 6a) to 1.23 (Figure 7a). The reduction is even more obvious on the south side of the model characterized by the q_{c1} parameter, where the critical factor of safety decreased from 1.58 in liquefaction analysis (Figure 6c) to 1.00 in post-liquefaction analysis (Figure 7c). This can be explained by the fact that the q_{c1} parameter indicates a higher volume of contractive zones than ψ and $Q_{tn,cs}$.

According to these results, models defined using the ψ and $Q_{tn,cs}$ parameters can satisfy the 1.2 target factor of safety on both sides of the model. The model classified by q_{c1} does not, however, meet the criterion. The critical surface on both sides of the model, as shown in Figure 7c, is localized, and limited to the TSF toe zone at elevations of 225 to 235 m on the south side and 230 to 235 m on the north side.

Adding a stabilizing berm on both sides of section B-B is suggested as a remedial design to increase the stability of TSF in terms of factor of safety on a preliminary basis. The berm could be placed at the first bench of the slope on the south side, at an elevation of 225 to 230 metres, and at an elevation of 230 to 235 metres on the north side. According to the TSF design, the berm width should be about 20 m. Figure 8 shows the similar configuration as

Figure 7c, except with the stabilizing berm on both sides of the model. As can be seen in this figure, the critical factor of safety has increased and both sides of the model have met the target factor of safety of 1.2. Although the use of the berm confirms an increase in TSF stability, the design of such structures requires additional considerations based on the TSF design and site constraints.

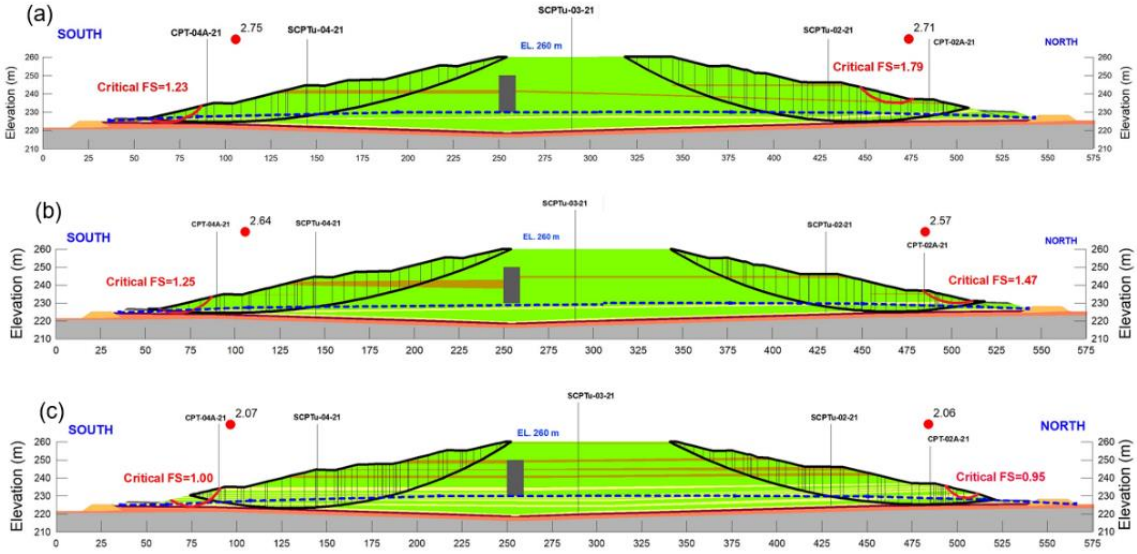

Figure 7. Post-Liquefaction stability results along the cross-section B-B with material zoning defined by (a) ψ, (b) $Q_{tn,cs}$, and (c) q_{c1} parameters

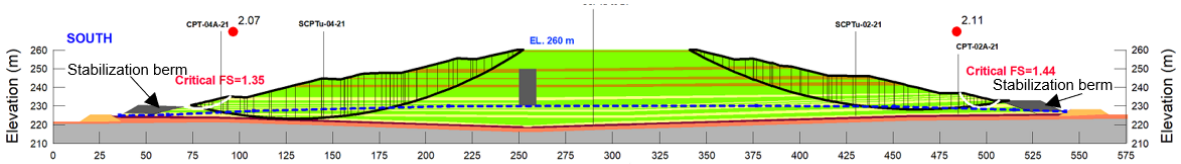

Figure 8. Post-Liquefaction stability result with stabilization berm along the cross-section B-B with material zoning defined by q_{c1}

6 CONCLUSION

In this study, the slope stability of the Éléonore Mine TSF - Phase 1 was evaluated to verify the stability with respect to static liquefaction. The classification of the tailings into contracting/dilating materials was performed using the three parameters, ψ, $Q_{tn,cs}$ and q_{c1}. The classification results show that contracting zones exist within the tailings pile. The extent of these contracting zones changes depending on the classification parameter (ψ, $Q_{tn,cs}$ and q_{c1}) used. However, the q_{c1} parameter predicted more contractive tailings zones in the TSF.

Liquefaction stability analysis against static liquefaction was performed using the limit equilibrium and Morgenstern-Price methods implemented in SLOPE/W software version 2021. These results show that the safety factor is greater than 1.5 in all cases.

To determine if the static shear forces exceed the available liquefied shear strength, post-liquefaction stability analyses were performed by assigning the residual undrained shear strength ratio ($\frac{Su_{(Liquified)}}{\sigma'_{v0}}$) to the layers most susceptible to liquefaction, which include all contractive layers beneath the water table and the first contractive layer above the water table. These results show that some sections are stable and have safety factors above the required factor of safety of 1.2, while others show potential instability. For the sections with safety factors lower than 1.2, corrective design measures may require a stabilizing berm on a preliminary basis with a height of ±5.0 m and a width of ±20 m. Considering these measures, the safety factors are all greater than 1.2 for section B-B. Given the fact that the placement of a berm increases the TSF stability, the construction of such structures necessitates additional considerations based on TSF design and site limitations.

7 REFERENCES

Bolton Seed, H., Tokimatsu, K., Harder, L. F., & Chung, R. M. 1985. Influence of SPT procedures in soil liquefaction resistance evaluations. Journal of geotechnical engineering, 111(12), 1425-1445.

Canadian Dam Association (CDA). 2013. Dam Safety Guidelines 2007 (2013 Edition)

Canadian Dam Association (CDA). 2019. Technical Bulletin: Application of Dam Safety Guidelines to Mining Dams 2014 (2019 Edition).

Canadian Dam Association (CDA). 2020. Technical Bulletin: Guidelines for Tailings Dam Breach Analyses.

Fear, C. E., and McRoberts, E. C. 1995. Report on liquefaction potential and catalogue of case histories. Internal Research Report, Geotechnical Engineering Library, Dept. of Civil Engineering, University of Alberta, Edmonton, Alberta, Canada, March (revision of September 1993 report).

Fear, C.E. & Robertson, P.K. 1995. Estimating the undrained strength of sand: A theoretical framework. Canadian Geotechnical Journal, v. 32:4, p. 859-870.

GEO-SLOPE International Ltd. 2012. Stability Modeling with SLOPE/W, An Engineering Methodology, November 2012 Edition.

Idriss, I. M., and Boulanger, R. W. 2008. Soil liquefaction during earthquakes. Monograph MNO-12, Earthquake Engineering Research Institute, Oakland, CA, 261 pp.

Boulanger, R. W., & Idriss, I. M. 2014. CPT and SPT based liquefaction triggering procedures. Report No. UCD/CGM.-14, 1.

Ishihara, K. 1993. Liquefaction and flow failure during earthquakes. *Géotechnique*, *43*(3), 351-451.

Jefferies, M. G., and Been, K. 2006. Soil liquefaction-A critical state approach, Taylor and Francis, London.

Jefferies, M.G., and Been, K. 2016. Soil liquefaction – a critical state approach. 2nd ed. Taylor & Francis. ISBN 0-419-16170-8.

Jefferies, M.G. and Davies, M.P.1991. “Soil classification by the cone penetration test: Discussion,” Canadian Geotechnical Journal, 28(1), pp. 173-176.

Ministère du Développement durable, de l’Environnement et des Parcs du Québec (MDDEP). 2012. Directive 019 sur l’industrie minière. Gouvernement du Québec.

Newmont. 2020b. Tailings Storage Facility (TSF) Technical & Operations Standard, Newmont Corporation, NEM-TSA-STA-017. October 2020.

Olson, S.M. 2001. Liquefaction Analysis of Level and Sloping Ground Using Field Case Histories and Penetration Resistance. Ph.D. Thesis, University of Illinois at Urbana-Champaign, Urbana III, 549 pp.

Olson, S. M., & Stark, T. D. 2003. Yield strength ratio and liquefaction analysis of slopes and embankments. Journal of Geotechnical and Geoenvironmental Engineering, 129(8), 727-737.

Pirete, W., & Gomes, R. C. 2013. Tailings liquefaction analysis using strength ratios and SPT/CPT results. Soils and Rocks, 36(1), 37-53.

Plewes, H.D., Davies, P., and Jefferies, M.G. 1992. CPT Based Screening Procedure for Evaluating Liquefaction Susceptibility. Proc., 45th Canadian Geotechnical Conf., Vol. 4, BiTech Publishers, Vancouver, BC, Canada, 1–9.

Poulos, S. J., Castro, G., & France, J. W. 1985. Liquefaction evaluation procedure. Journal of Geotechnical Engineering, 111(6), 772-792.

Rauch, A. F. 1997. An empirical method for predicting surface displacements due to liquefaction-induced lateral spreading in earthquakes (Doctoral dissertation, Virginia Tech).

Robertson, P. K., and Wride, C. E. 1998. ‘‘Evaluating cyclic liquefaction potential using the cone penetration test.’’ Can. Geotech. J., Ottawa, 35(3), 442–459.

Robertson, P.K. 2010. Evaluation of flow liquefaction and liquefied strength using the Cone Penetration Test. Journal of Geotechnical & Geoenvironmental Engineering, Vol. 136(6), 842-853.

Robertson, P.K. 2016. Cone penetration test (CPT)-based soil behaviour type
(SBT) classification system — an update. Canadian Geotechnical Journal,
53(12): 1910–1927. doi:10.1139/cgj-2016-0044.

Robertson, P. K. 2022. Evaluation of flow liquefaction and liquefied strength using the cone penetration test: an update. Canadian Geotechnical Journal, 59(4), 620-624.

Shuttle, D. A., and Cunning, J. 2007. Liquefaction potential of silts from CPTu.” Can. Geotech. J., 44, 1–19.

Zhang, G., Robertson, P.K. and Brachman, R.W.I. 2002. Estimating Liquefaction induced Ground Settlements from CPT for Level Ground, Canadian Geotechnical Journal, 39(5): 1168-1180.